AD-A195 398 ENSEMBLE MONTE CARLO SIMULATION OF A VELOCITY-MODULATION FIELD EFFECT TRA..(U) ILLINOIS UNIV AT URBANA COORDINATED SCIENCE LAB 1/1

UNCLASSIFIED I C KIZILYALLI ET AL. SEP 87 F/G 9/1 NL

END
DATE FILMED
8 88

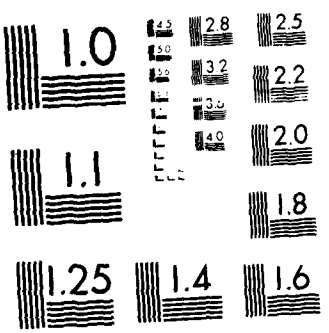

SECURITY CLASSIFICATION OF THIS PAGE

REPORT DOCUMENTATION PAGE

(2)

AD-A195 398

DTIC FILE COPY

ELECTE MAY 17 1988 S D

1a. REPORT SECURITY CLASSIFICATION: Unclassified	1b. RESTRICTIVE MARKINGS: None
2a. SECURITY CLASSIFICATION AUTHORITY	3. DISTRIBUTION/AVAILABILITY OF REPORT: Approved for public release; distribution unlimited
2b. DECLASSIFICATION/DOWNGRADING SCHEDULE	
4. PERFORMING ORGANIZATION REPORT NUMBER(S): Reprint	5. MONITORING ORGANIZATION REPORT NUMBER(S): ARO 24094.14-EL
6a. NAME OF PERFORMING ORGANIZATION: Coordinated Science Lab, University of Illinois; 6b. OFFICE SYMBOL (If applicable): N/A	7a. NAME OF MONITORING ORGANIZATION: U.S. Army Research Office
6c. ADDRESS (City, State, and ZIP Code): 1101 W. Springfield Avenue, Urbana, IL 61801	7b. ADDRESS (City, State, and ZIP Code): P.O. Box 12211, Research Triangle Park, NC 27709-2211
8a. NAME OF FUNDING/SPONSORING ORGANIZATION: U.S. Army Research Office; 8b. OFFICE SYMBOL (If applicable)	9. PROCUREMENT INSTRUMENT IDENTIFICATION NUMBER: DAAL 03-86-K-0099
8c. ADDRESS (City, State, and ZIP Code): P.O. Box 12211, Research Triangle Park, NC 27709-2211	10. SOURCE OF FUNDING NUMBERS: PROGRAM ELEMENT NO. / PROJECT NO. / TASK NO. / WORK UNIT ACCESSION NO.

11. TITLE (Include Security Classification)

Ensemble Monte Carlo Simulation of a Velocity-Modulation Field Effect Transistor (VMT)

12. PERSONAL AUTHOR(S): Kizilyalli, I. C. and Hess, K.

13a. TYPE OF REPORT	13b. TIME COVERED	14. DATE OF REPORT (Year, Month, Day)	15. PAGE COUNT
Technical	FROM _____ TO _____	1987 September	6

16. SUPPLEMENTARY NOTATION: The view, opinions and/or findings contained in this report are those of the author(s) and should not be construed as an official Department of the Army position, policy, or decision, unless so designated by other documentation.

17. COSATI CODES			18. SUBJECT TERMS (Continue on reverse if necessary and identify by block number)
FIELD	GROUP	SUB-GROUP	velocity, modulated field effect transistors; Monte Carlo methods. (Reprints)

19. ABSTRACT (Continue on reverse if necessary and identify by block number)

We present numerical simulations of velocity modulated field-effect transistors as proposed by Sakaki. Using self-consistent particle-field Monte Carlo analysis, we assess possible advantages of these novel device structures with respect to switching speed and show the qualitative correctness of Sakaki's ideas. Quantitatively, delays are introduced by the redistribution of electrons in the separated channels.

20. DISTRIBUTION/AVAILABILITY OF ABSTRACT	21. ABSTRACT SECURITY CLASSIFICATION
☒ UNCLASSIFIED/UNLIMITED ☐ SAME AS RPT. ☐ DTIC USERS	Unclassified
22a. NAME OF RESPONSIBLE INDIVIDUAL	22b. TELEPHONE (Include Area Code) / 22c. OFFICE SYMBOL

DD FORM 1473, 84 MAR — 83 APR edition may be used until exhausted. All other editions are obsolete.

SECURITY CLASSIFICATION OF THIS PAGE

UNCLASSIFIED

Reprinted from
JAPANESE JOURNAL OF APPLIED PHYSICS
VOL. 26, No. 9, September, 1987, pp. 1519-1524

Ensemble Monte Carlo Simulation of a Velocity-Modulation Field Effect Transistor (VMT)

I. C. KIZILYALLI and K. HESS

Coordinated Science Laboratory and
Department of Electrical and Computer Engineering,
University of Illinois, Urbana, Illinois 61801 U.S.A.

JAPANESE JOURNAL OF APPLIED PHYSICS
Vol. 26, No. 9, September, 1987, pp. 1519-1524

Ensemble Monte Carlo Simulation of a Velocity-Modulation Field Effect Transistor (VMT)

I. C. KIZILYALLI and K. HESS

Coordinated Science Laboratory and
Department of Electrical and Computer Engineering,
University of Illinois, Urbana, Illinois 61801 U.S.A.

(Received March 11, 1987; accepted for publication May 23, 1987)

We present numerical simulations of velocity modulated field effect transistors as proposed by Sakaki. Using self-consistent particle-field Monte Carlo analysis, we assess possible advantages of these novel device structures with respect to switching speed and show the qualitative correctness of Sakaki's ideas. Quantitatively, delays are introduced by the redistribution of electrons in the separated channels.

§1. Introduction

In field effect transistors, the source to drain current is controled by modulating the charge carrier concentration under the gate. Therefore, the ultimate switch-on time is roughly determined by the transit time of electrons from source to drain. The calculated switch-on time for a 0.4 micrometer gate length (1 micrometer from source to drain) high-electron mobility transistor is longer than 3.5 picoseconds at 300 K,[1,2] and about 3.2 picoseconds at 77 K.

To achieve sub-picosecond switching in semiconductors, Sakaki proposed the concept of velocity-modulation transistors (VMT's).[3,4] The velocity-modulation transistor concept attempts to capitalize on the extremely short perpendicular transit times between two adjacent channels, with different transport properties (i.e., mobility). The original structure suggested by Sakaki is a n-AlGaAs/GaAs/n-AlGaAs double heterostructure (Fig. 1).[3] Two channels are formed at the heterointerfaces in GaAs. One of the channels is heavily doped with acceptors and donors, and therefore exhibits a low mobility, while the other channel, the high mobility channel, is undoped. Schottky barriers are placed on top and bottom of the device to switch the electrons back and forth perpendicular to the interface, hence modulating the mobility and current between the source and drain.

If it is assumed that the intrinsic device speed is limited by the perpendicular transit time, the switching time can be estimated as follows. For a channel separation of 500 Å, and a velocity of 1×10^{7} cm/s (ignoring velocity) overshoot) perpendicular to the heterointerface, the switching time can be estimated as $\tau\simeq0.5$ picoseconds. This is an order of magnitude faster than common switching times which involve the gate length.[3,4]

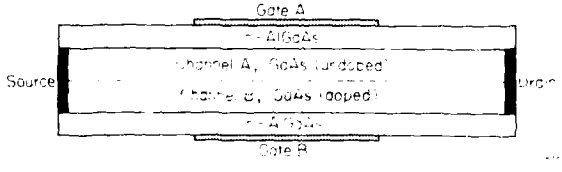

Fig. 1. Device topology of the velocity-modulation transistor (VMT) as proposed by Sakaki.

The dynamics of electron transfer between two adjacent equivalent high mobility channels (dual-channel high-electron mobility transistor) were previously reported for 300 K operation.[2,5] It has been concluded that the ideas of multiple channel transfer are valid, and ultimate device speeds could be enhanced if these ideas can be realized. However, it also has been found that the electron redistribution along the device channel plays an important role and prolongs the time period which is necessary to reach steady state, even if the electrons are switched perpendicular to the layers rather fast.

The purpose of this paper is to discuss the factors influencing the time constants of a velocity-modulation transistor, at 77 K and 300 K. We will elaborate on the ultimate device speed, on-state and off-state current levels, time evolution of the electron distribution function, and ionized impurity scattering as a means to modulate channel mobility of a field effect transistor.

§2. Device Structure and Simulation

The structure used in the simulations in an n-AlGaAs/GaAs/n-AlGaAs double heterostructure as shown in Fig. 2. The AlGaAs layers are doped relatively lightly ($N_D=2\times10^{17}$ cm^{-3}, where N_D is the donor concentration). The two channels (A and B) formed at the heterointerface are assumed to be contacted separately. Channel B is assumed to be undoped ($N_D=1\times10^{15}$ cm^{-3}) and channel A is heavily doped with both acceptors and donors present in order to reduce the mobility. Schottky barriers are placed on top and bottom of the device to modulate the conductivity of the channels. The thickness of the GaAs is chosen to be 1000 Å. Under these circumstances size quantization effects are unimportant and our

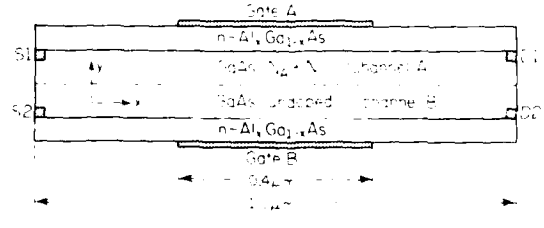

Fig. 2. Device topology of the structure simulated.

semiclassical treatment is appropriate. The source to drain distance is 1 micrometer and the gates are symmetrically placed between source and drain and are 0.4 micrometers long.

Our Monte Carlo model incorporates the Γ-L-X band structure for both GaAs and AlGaAs. Polar optical phonon sattering, equivalent and non-equivalent intervalley scattering, real space transfer, impact ionization and ionized impurity scattering are included in the model which has been described in detail previously.[2,6]

The total number of sample electrons in the device is a variable, and the electron population is allowed to adjust itself to satisfy overall charge neutrality. Small regions surrounding the ohmic contacts are kept neutral by injecting electrons chosen from an equilibrium energy distribution as needed. The source and drain currents are determined by recording the number of injected and absorbed particles during a preset time interval.[7,8]

The electric field distribution in the device domain is updated every time step (2 femtoseconds) by solving Poisson's equation numerically by the finite difference method and successive over relaxation. Dirichlet conditions are imposed at the metal-semiconductor surfaces, and potential continuity conditions are used at the AlGaAs/GaAs interface. The perpendicular field changes as the ratio of the dielectric constants.

§3. Results

3.1 *Switching times*

We first present the switching time simulations for 300 K operation. The device is initially ($t=0$) in its off-state as shown in Fig. 3(a). The current is carried by electrons in the low mobility channel (channel A). The gate voltage of channel A is 0.6 volts, and the gate voltage of channel B is 0.0 volts. Source voltages are kept at 0.0 volts and the drain voltages are kept 0.8 in all of the simulations. To switch the device on, the gate voltage of channel A is instantaneously decreased to 0.0 volts, and the gate voltage of channel B is instantaneously increased to 0.6 volts. Channel A is immediately fully depleted (Figs. 3(b) and 3(c)). The transit time for perpendicular transport (from one interface to the other) is completed in about 0.2 picoseconds, regardless of the doping profiles. However, steady state is only completely reached after the electrons that are transferred to the high mobility channel (channel B) redistribute themselves to achieve normal channel conduction. This redistribution takes 2.0 to 3.0 picoseconds, depending on the ionized impurity concentration of the low mobility channel ((Fig. 3(d)).

The switch-off simulation starts from the steady state on-configuration (Fig. 3(d)). The gate voltages of channel A and B are instantaneously reversed as shown in Figs. 4(a) and 4(b). The electrons are transferred to channel A again in about 0.2 picoseconds. However, steady state is reached only after 2.5 to 2.8 picoseconds depending on the ionized impurity concentration in the low mobility channel (Figs. 5(a)-5(d)), again because of the redistribution of electrons in the given channel.

We have defined steady state as the point of operation where the drain and source currents have stabilized and are within 10% of each other. After 0.2 picoseconds,

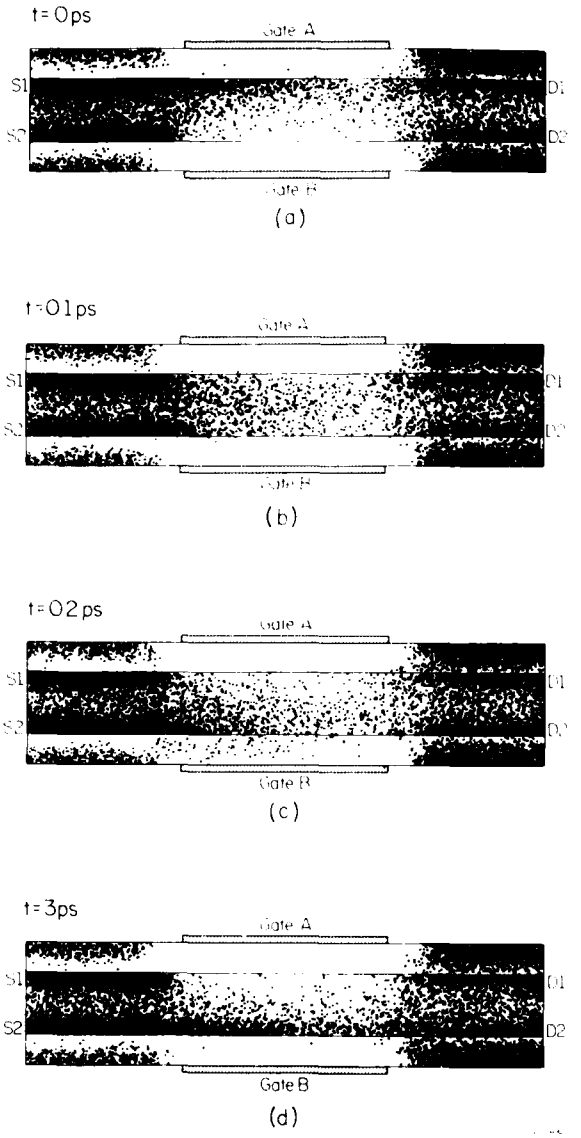

Fig. 3. Electron transfer behavior during switch-on transient at, (a) $t=0$ picoseconds, (b) $t=0.1$ picoseconds, (c) $t=0.2$ picoseconds, (d) $t=3$ picoseconds.

which is the perpendicular transit time, source and drain current levels can be a factor of two apart from each other, or their respective steady state values. We conclude therefore that the intrinsic device speed is not only limited by the perpendicular transit time.

The switch-on and switch-off times which are necessary to reach steady state at 300 K and 77 K for various dopings of channel A are summarized in Table I. The switch-on and switch-off times calculated for the velocity-modulation transistor (VMT) are shorter than for longitudinal (source-to-drain) switch-on times which are 3.5 and 3.2 picoseconds for 300 K and 77 K respectively.

Increasing the impurity concentrations leads to longer switch-on and switch-off times. The calculations also show that switch-off is always faster than switch-on. We comment on this point in the discussion section.

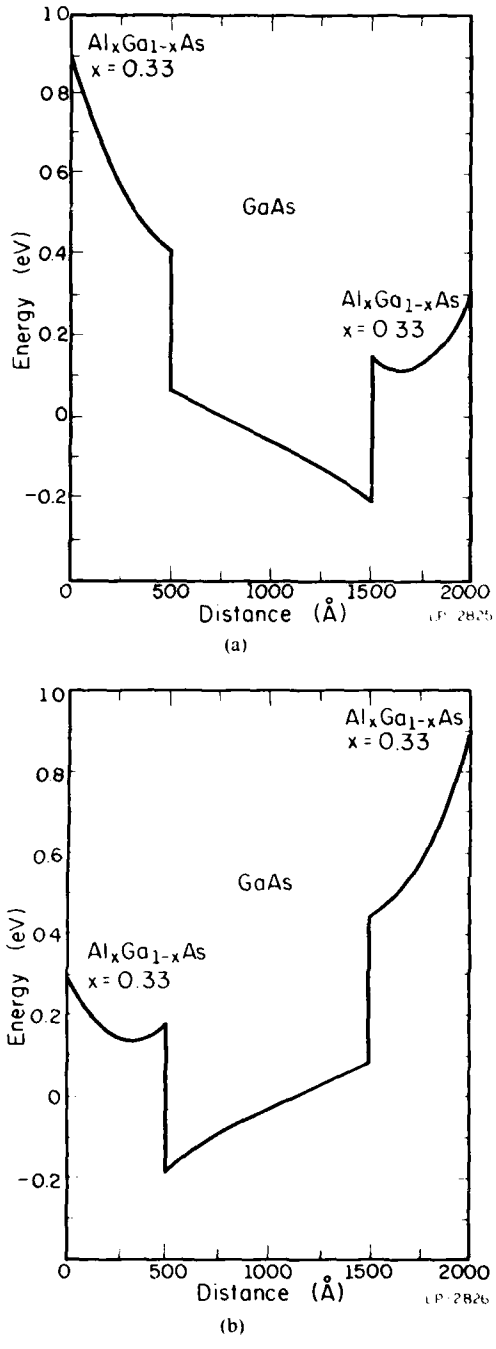

Fig. 4. The energy band profile of the structure across the gates (at $x=0.5$ micrometers) for two different biasing conditions. (a) $V_{GA}=0.0$ V, $V_{GB}=0.6$ V, (b) $V_{GA}=0.6$ V, $V_{GB}=0.0$ V.

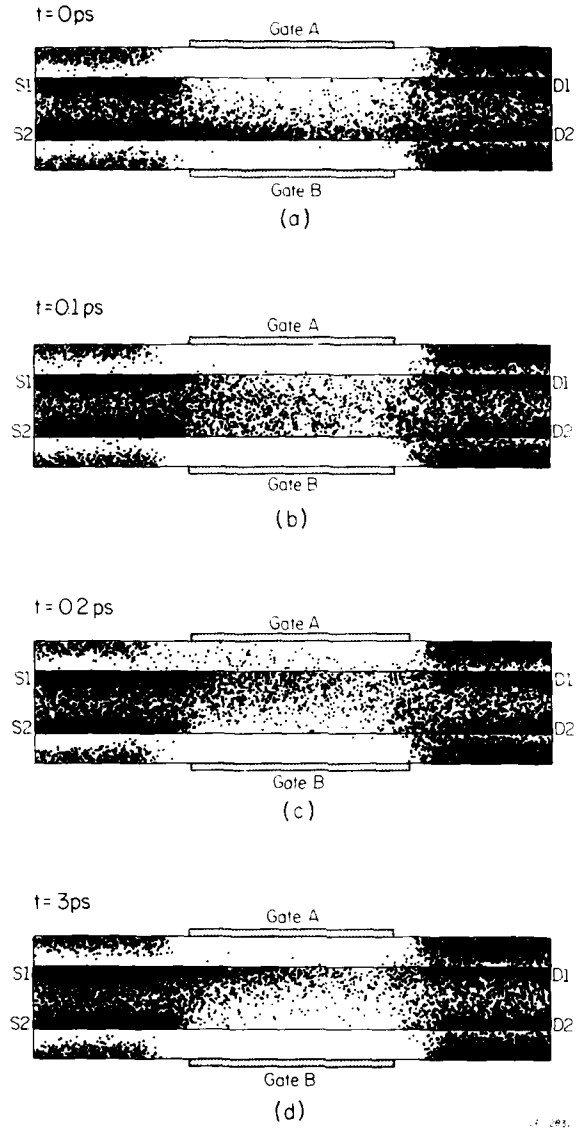

Fig. 5. Electron transfer behavior during switch-off transient at, (a) $t=0$ picoseconds, (b) $t=0.1$ picoseconds, (c) $t=0.2$ picoseconds, (d) $t=3$ picoseconds.

3.2 *Evolution of the electron distribution function*

The electron energy distribution function cannot directly be measured but is important for the understanding of the device. The study of its time evolution shows clearly that the intrinsic device speed is not only limited by the perpendicular transit time (0.2 picoseconds), but also by the lateral distribution of electrons.

For the biasing conditions considered in this paper, the electrons in the device channel are mostly in the Γ-valley, except at the drain edge of the gate (pinch-off region). Therefore only the Γ-valley electrons in GaAs, under the gate region of the device will be described in detail.

Table 1.

Channel A doping	τ_{on} (300 K)	τ_{on} (77 K)	τ_{off} (300 K)	τ_{off} (77 K)
$N_A=0$ $N_D=1\times10^{15}$ cm^{-3}	2.0 ps	(—)	2.0 ps	(—)
$N_A=2\times10^{17}$ cm^{-3} $N_D=2.01\times10^{17}$ cm^{-3}	3.0 ps	(—)	2.8 ps	(—)
$N_A=2\times10^{18}$ cm^{-3} $N_D=2.001\times10^{18}$ cm^{-3}	3.0 ps	2.4 ps	(2.8–3.0) ps	2.3 ps

Initially ($t=0^-$), the electrons are in the low mobility channel, and are at steady state (Fig. 6(a)). The displacement of the distribution function in the k_x direction (parallel to the interface) indicates some current flow from source to drain in the device. When the gate biases are reversed ($V_{GA}=0.0$ volt, $V_{GB}=0.6$ volts at $t=0^+$), the

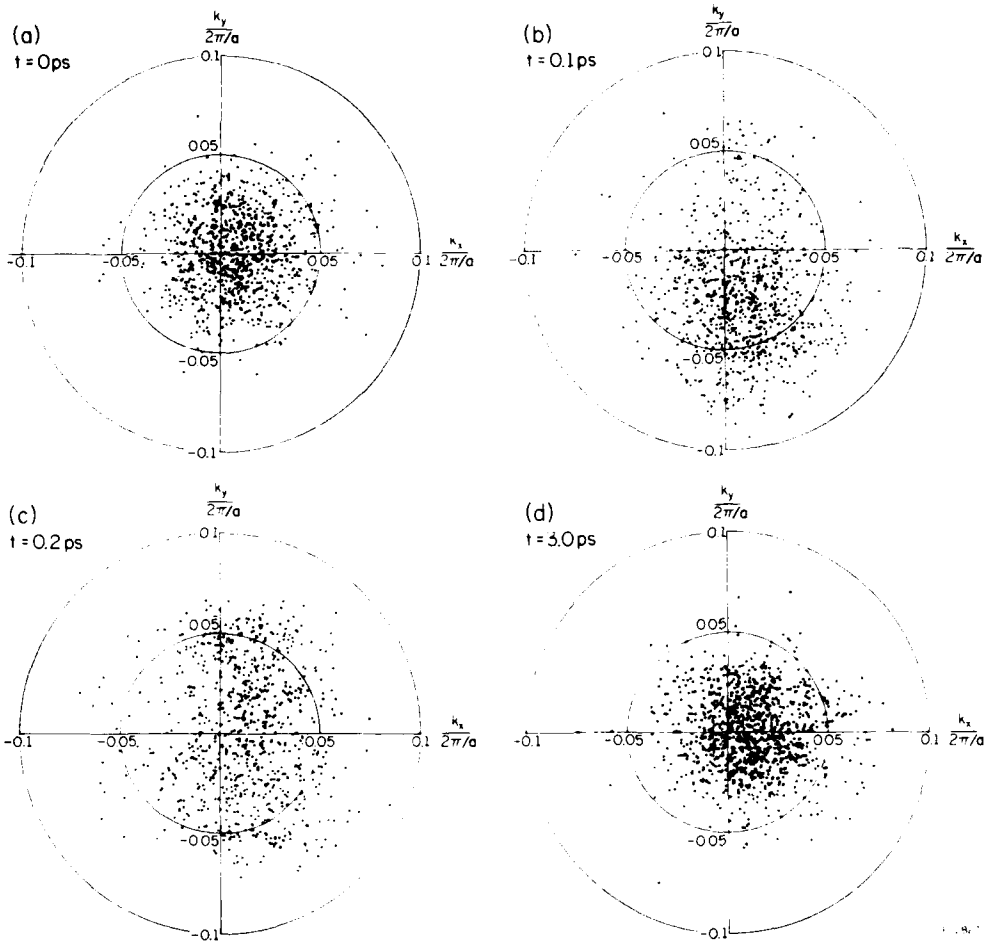

Fig. 6. Evolution of the electron distribution function under the gates during switch-on transient at, (a) $t=0$ picoseconds, (b) $t=0.1$ picoseconds, (c) $T=0.2$ picoseconds, (d) $t=3$ picoseconds.

electron distribution function is shifted into the $-k_z$ (perpendicular to the heterointerface) direction (Fig. 6(b)). Electrons impinging on the interface are reflected back into GaAs if they cannot surmount the potential barrier. Therefore the first quadrant of k-space is populated (Fig. 6(c)). Steady state is reached sometime after the electrons have transferred to the high mobility channel (Fig. 6(d)).

The evolution of the electron distribution function during the switch-off transient is shown in Figs. 7(a)-7(d).

It is observed that the transient and steady state distribution functions are not spherically symmetric. This deviation from a Maxwell-Boltzmann distribution follows from the dependence of the scattering rates on the particle momentum, and energy exchange between electrons and polar phonons in GaAs.

3.3 *Current levels*

In the operation of the velocity-modulation transistor, an increase in source-to-drain current is expected as the electrons are moved to the high mobility channel. The current switch-on transient at 77 K is shown in Fig. 8. The off-state current is $I_{OFF}=32$ mA/mm (at $t=0$). After 0.2 picoseconds (perpendicular transit time of electrons) the source and drain currents have not yet reached steady state, which is reached in ≈ 2.4 picoseconds and the on-state current is $I_{ON}=98$ mA/mm.

At 300 K, a current of $I_{ON}=80$ mA/mm flows through the VMT when it is in on-state. The "off-state" current is, $I_{OFF}=49$ mA/mm for a heavily doped low mobility channel ($N_A=2\times10^{18}$ cm^{-3}, $N_D=2.001\times10^{18}$ cm^{-3}).

Therefore, the channel current can be modulated by $\approx 40\%$ at 300 K, and by $\approx 70\%$ at 77 K, if a highly compensated concentration of ionized impurities is introduced into the device channel.

3.4 *Average electron velocity distribution*

The average electron velocity along the device channel is sketched for 300 K in Fig. 9, and for 77 K in Fig. 10 for various channel dopings.

The velocity distribution profiles for all channel doping have the same qualitative form. The electrons entering the high electric field region at the drain side of the gate, experience velocity overshoot.[9] The peak electron velocities are 4.1×10^7 cm/s at 300 K, and 6.3×10^7 cm/s at 77 K. The average electron velocities in the low electric field regions of the device are much lower. The effect of the ionized impurities on the velocity distribution profile is more prominent at lower temperatures, especially in the low electric field regions (i.e., source-to-gate) of the

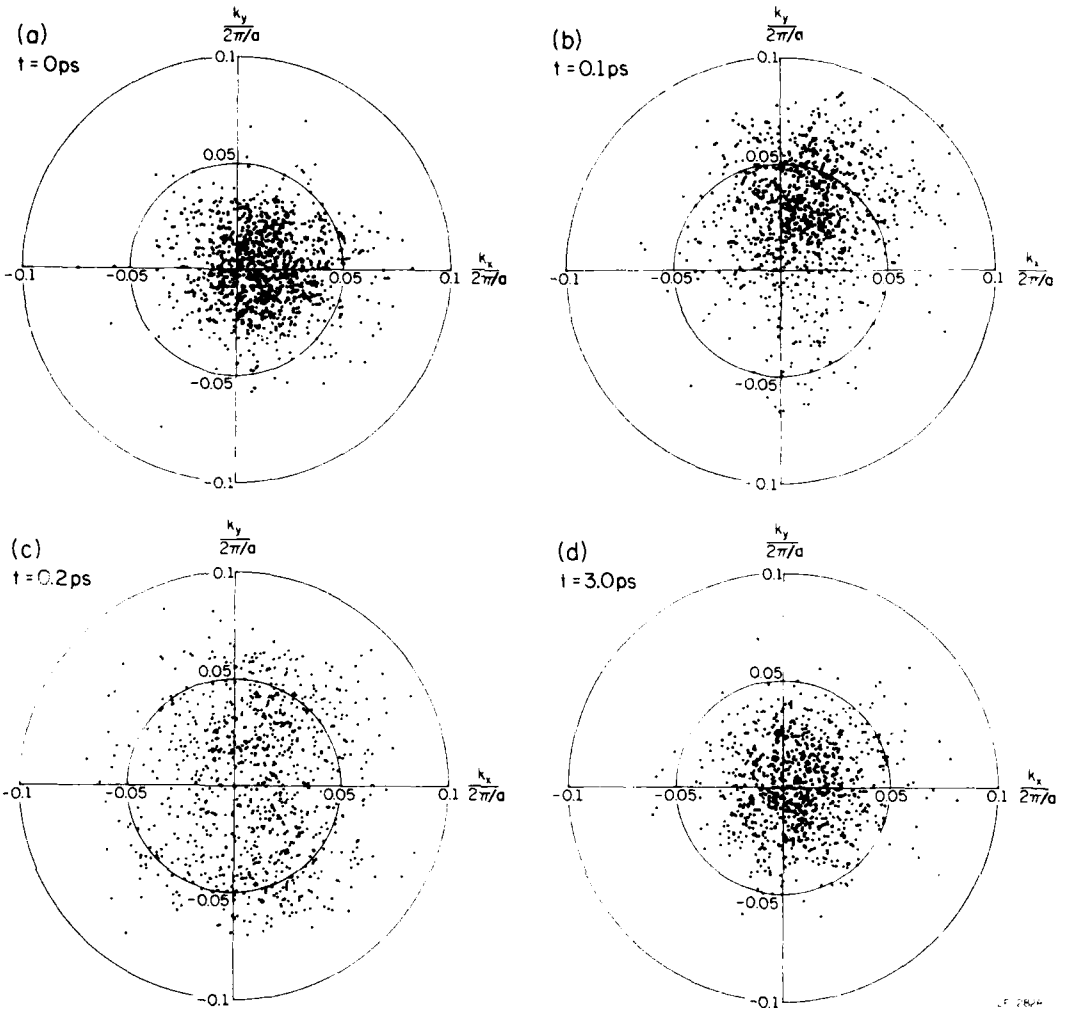

Fig. 7. Evolution of the electron distribution function under the gates during switch-off transient at, (a) $t=0$ picoseconds, (b) $t=0.1$ picoseconds, (c) $t=0.2$ picoseconds, (d) $t=3$ picoseconds.

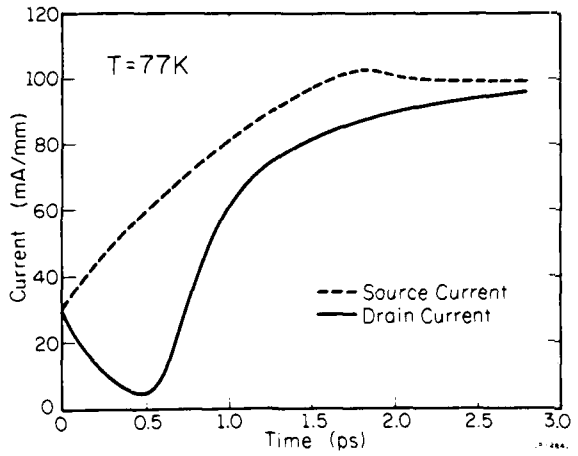

Fig. 8. Current switch-on transient for the velocity-modulation transistor at 77 K.

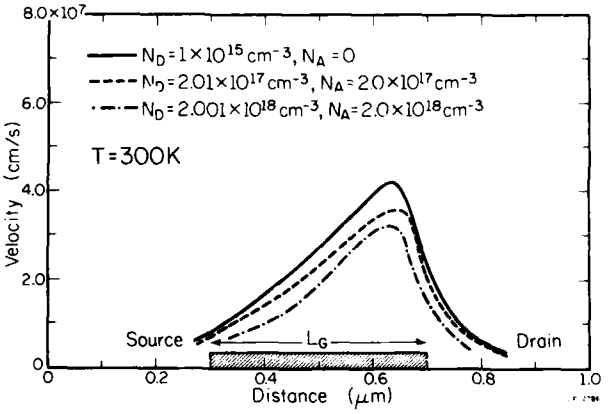

Fig. 9. Average electron velocity in undoped and heavily doped channels of the velocity-modulation transistor at 300 K.

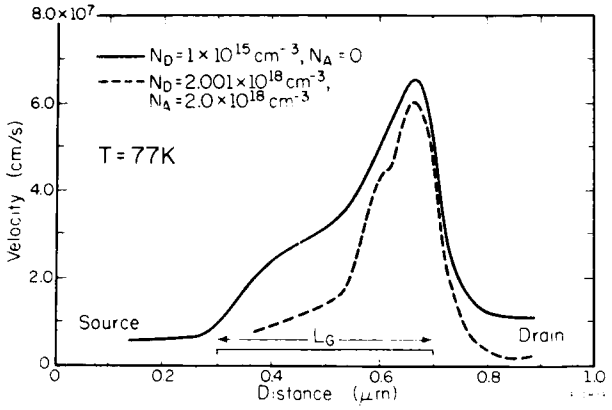

Fig. 10. Average electron velocity in undoped and heavily doped channels of the velocity-modulation transistor at 77 K.

device. This is due to the increased ionized impurity scattering rate at lower temperature and lower average electron energies.

§4. Discussion

The calculations presented above show that the current through a device can be reduced by 40% at 300 K and 70% at 77 K if electrons are transferred from a high mobility channel to a highly doped compensated channel with $N_D = 2.001 \times 10^{18}\ \text{cm}^{-3}$ and $N_A = 2 \times 10^{18}\ \text{cm}^{-3}$. However, the reduction in electron velocity distribution in the device under the gate is at most 30% at 300 K, and 60% at 77 K. Therefore velocity reduction alone does not explain the total change in channel conductance. An investigation of the electron distribution in the conducting channels of the device (Fig. 3(a) and Fig. 5(a)) reveals that there are more carriers in the channel when the device is in its on-state (Fig. 5(a)). In fact, the concentration of electrons in the channel is increased by about 15% when the device is switched on.

Change in the carrier concentration under the gate is brought about by the different source resistances and field distributions, depending upon whether the electrons are in undoped or heavily doped channel. The difference in the source resistances can be explained from the energy dependence of impurity scattering. As it is well known, ionized impurity scattering prefers small scattering angles, especially at higher electron energies.[10] Therefore ionized impurity scattering is most important in determining mobilities in the low electric field regions of the device, i.e., the source to gate region. This difference in source resistances is sufficient to explain the higher electron concentrations under the gate when the channel is undoped.

Finally we would like to comment on the observed asymmetry between switching on and off. The calculated switch-on times are always larger than switch-off times. This is a general property of the field effect transistors and in this case also a consequence of the symmetric gate biases used for switching here. As mentioned above, change in the channel conductance is due to two factors; change in electron mobility and electron concentration ($\Delta G = n\Delta\mu + \mu\Delta n$, where ΔG is the change in channel conductance, $\Delta\mu$ is the difference in mobility between the channels, and Δn is the difference in electron concentration under the gate). To switch the VMT on, by simply reversing the gate biases will bring in more electrons (~15% more than what has been transferred from the low mobility channel) from the source and drain contact. To switch the VMT off, electrons are transferred to the low mobility channel and any excess electrons are disposed of through the source and drain, i.e., excess carriers need not transit the total source to drain (or at least gate) length.

This suggests that switch-on and switch-off times can be reduced further (to about 2 ps at 300 K) if slightly asymmetric gate biases which force the condition $\Delta n = 0$, for the operation of the VMT are used. However, this will be at the expense of a smaller modulation in the channel conductance.

§5. Conclusions

The velocity modulation field effect transistor has been studied by self-consistent particle-field Monte Carlo methods.

This study shows that current switching can be achieved by the velocity modulation concept.

The perpendicular transport of electrons between the two channels is achieved in extraordinarily short times (≈0.2 picoseconds). This is due to short distances involved between the channels (1000 Å), and very high average electron velocities ($4\text{–}6 \times 10^7$ cm/s) perpendicular to the interface. However, the necessary interface charge readjustment takes much longer than perpendicular transport, and is accomplished only in times comparable to the longitudinal (source-to-drain) switch-on time. With the proper choice of gate biases the switching speed of the VMT's will be superior to that of the conventional GaAs field effect transistors. We estimated speed up of abut 1.5 picoseconds for 1 micrometer (0.4 micrometer gate length) device.

Acknowledgement

The authors would like to thank Mike Artaki, Tahui Wang, and Kiyoyuki Yokoyama for discussions in the early stages of this work. This work was supported by the Army Research Office and Joint Services Electronics Program.

References

1) I. C. Kizilyalli, K. Hess, J. L. Larson and D. J. Widiger: IEEE Trans. on Electron Devices, ED-33 (1986) 1427.
2) I. C. Kizilyalli, K. Hess and G. J. Iafrate: J. Appl. Phys. 61 (1987) 2395.
3) H. Sakaki: Jpn. J. Appl. Phys. 21 (1982) L381.
4) K. Hirakawa, H. Sakaki and J. Yoshino: Phys. Rev. Lett. 54 (1985) 614.
5) I. C. Kizilyalli, K. Hess, G. J. Iafrate and D. Smith: NUMOS I (International Conference on the Numerical Modeling of Semiconductors), Los Angeles, Dec. 11-12 (1986).
6) T. Wang and K. Hess: J. Appl. Phys. 57 (1985) 5336.
7) R. Castagne: Physica, 134B & C (1985) 55.
8) C. Moglestue: IEEE Trans. Electron Devices ED-32 (1985) 2092.
9) E. Constant: *Hot-Electron Transport in Semiconductors*, ed. L. Reggiani (Springer-Verlag, New York, 1984) Chap. 8.
10) J. G. Ruch and W. Fawcett: J. Appl. Phys. 41 (1970) 3843.